DEVELOPMENT

A microtubule-organizing center directing intracellular transport in the early mouse embryo

J. Zenker,[1] M. D. White,[1] R. M. Templin,[2] R. G. Parton,[2] O. Thorn-Seshold,[3] S. Bissiere,[1] N. Plachta[1,4]*

The centrosome is the primary microtubule-organizing center (MTOC) of most animal cells; however, this organelle is absent during early mammalian development. Therefore, the mechanism by which the mammalian embryo organizes its microtubules (MTs) is unclear. We visualize MT bridges connecting pairs of cells and show that the cytokinetic bridge does not undergo stereotypical abscission after cell division. Instead, it serves as scaffold for the accumulation of the MT minus-end–stabilizing protein CAMSAP3 throughout interphase, thereby transforming this structure into a noncentrosomal MTOC. Transport of the cell adhesion molecule E-cadherin to the membrane is coordinated by this MTOC and is required to form the pluripotent inner mass. Our study reveals a noncentrosomal form of MT organization that directs intracellular transport and is essential for mammalian development.

Microtubules (MTs) establish a wide range of spatial configurations critical for various cellular functions including cell division, differentiation, and morphogenesis. Outgrowth of MTs by nucleation is initiated at microtubule-organizing centers (MTOCs), which are sites that stabilize or anchor MT minus ends (*1*). In most animal cells, the centrosome serves as the main MTOC (*2*). However, preimplantation embryos develop until the mid-blastocyst stage (64 cells) before assembling centrosomes (*3*, *4*). Therefore, it remains unclear how MTs are spatially organized during early mammalian development (*5*, *6*). Beyond centrosomes, MTs can also grow from noncentrosomal sites containing CAMSAPs (calmodulin-regulated spectrin-associated proteins), which stabilize MT minus ends (*1*, *7*, *8*). Yet it is not known whether this mechanism of MT organization exists in the early mammalian embryo.

To reveal MT organization during early development, we imaged live mouse embryos expressing fluorescently labeled MT-associated protein MAP2c. Our movies demonstrate the persistence of MT bridges connecting pairs of cells, from the two-cell stage to the blastocyst stage (Fig. 1, A and C; fig. S1A; and movies S1 and S2). Bridge-like structures were previously observed using tubulin staining in fixed preimplantation human and mouse embryos, yet their functions remain unknown (*9*–*11*).

During cell division in most cell types, a stereotypical cytokinetic bridge forms between the sister cells, and this bridge is abscised shortly after cytokinesis (*12*). However, in the early embryo, the bridge connects each sister cell pair throughout most of interphase (Fig. 1, fig. S1, and movies S1 to S3). This interphase bridge maintains MT plus ends labeled by the end-binding proteins EB1 and EB3, as well as stembody markers including aurora B (fig. S2). Yet in contrast to the MTs of a stereotypical cytokinetic bridge that align predominantly from the cell nucleus to the stembody, the MTs of the interphase bridge project more broadly throughout the cell (fig. S3A). Moreover, when a cell enters mitosis, the depolymerization of its MT network is propagated along the interphase bridge toward the connected sister cell, which then enters mitosis (fig. S3, B to D, and movie S3).

Ablation of the interphase bridge using a femtosecond laser causes depolymerization of its MTs within ~60 s (Fig. 2A). Subsequently, the overall MT density within both sister cells decreases, and they adopt a more spherical cell shape (Fig. 2, B and C; fig. S4; and movie S4). Because ablation of MTOCs in other systems produced comparable widespread MT depolymerization (*13*–*16*), we hypothesized that the interphase bridge could function as an MTOC in the mouse embryo. Tracking the MT plus-end marker EB3-dTomato to visualize MT outgrowth (*17*) shows that, at the cytokinetic bridge, 98.6 ± 1.4% of MT plus ends project in a cell-to-bridge direction (Fig. 2D and movie S5). By contrast, at the interphase bridge, 77.7 ± 2.5% of EB3-dTomato tracks follow the opposite trajectory, demonstrating extensive MT outgrowth from the interphase bridge into the cell (Fig. 2E and movie S5).

Nocodazole treatment causes extensive loss of MTs. However, the interphase bridges are spared (fig. S5A), similar to the high resistance of centrosomes to nocodazole in other cell types (*18*). Furthermore, following nocodazole washout, these spared bridges resume MT outgrowth, and the cells rebuild a MT network (fig. S5, A and B, and movie S6). Similarly, after cold treatment, MT recovery is prominent near the interphase bridge (fig. S5C). MT outgrowth from the interphase bridge can also be optically inhibited with the use of 405-nm light, in live embryos cultured with

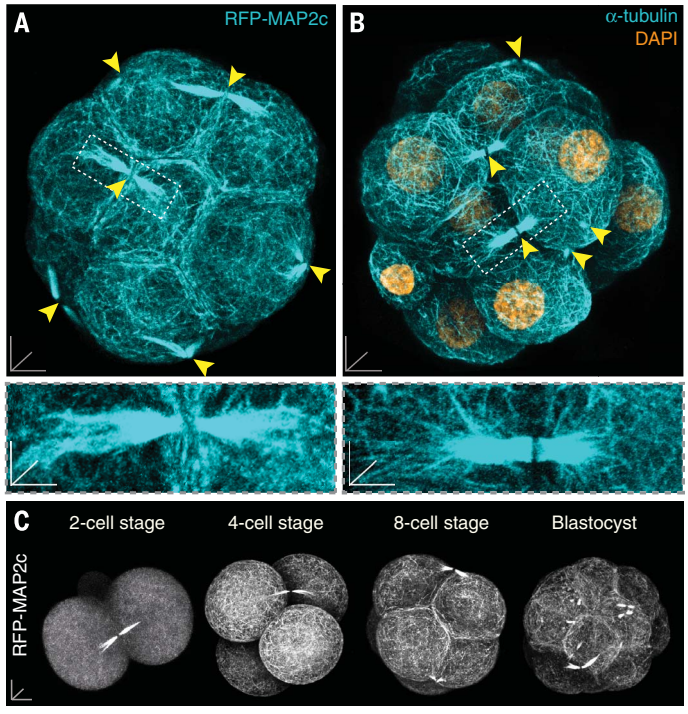

Fig. 1. Interphase MTs are organized in the early mouse embryo. (**A**) Live embryo shows MT bridges (arrowheads) connecting pairs of cells in interphase. (**B**) α-tubulin and DAPI (4′,6-diamidino-2-phenylindole) staining reveals comparable structures in a fixed embryo. For (A) and (B), insets show a zoomed-in view of the areas outlined by the dashed rectangles. (**C**) Live-embryo imaging demonstrates MT interphase bridges at multiple developmental stages. RFP, red fluorescent protein. Scale bars, 10 μm; 2 μm in insets.

[1]Institute of Molecular and Cell Biology, Agency for Science, Technology and Research (A*STAR), Singapore. [2]Institute for Molecular Biosciences and Centre for Microscopy and Microanalysis, University of Queensland, Brisbane, Queensland, Australia. [3]Department of Pharmacy, Center for Drug Research, Ludwig-Maximilians-University Munich, Munich, Germany. [4]Department of Biochemistry, Yong Loo Lin School of Medicine, National University of Singapore, Singapore.
*Corresponding author. Email: plachtan@imcb.a-star.edu.sg

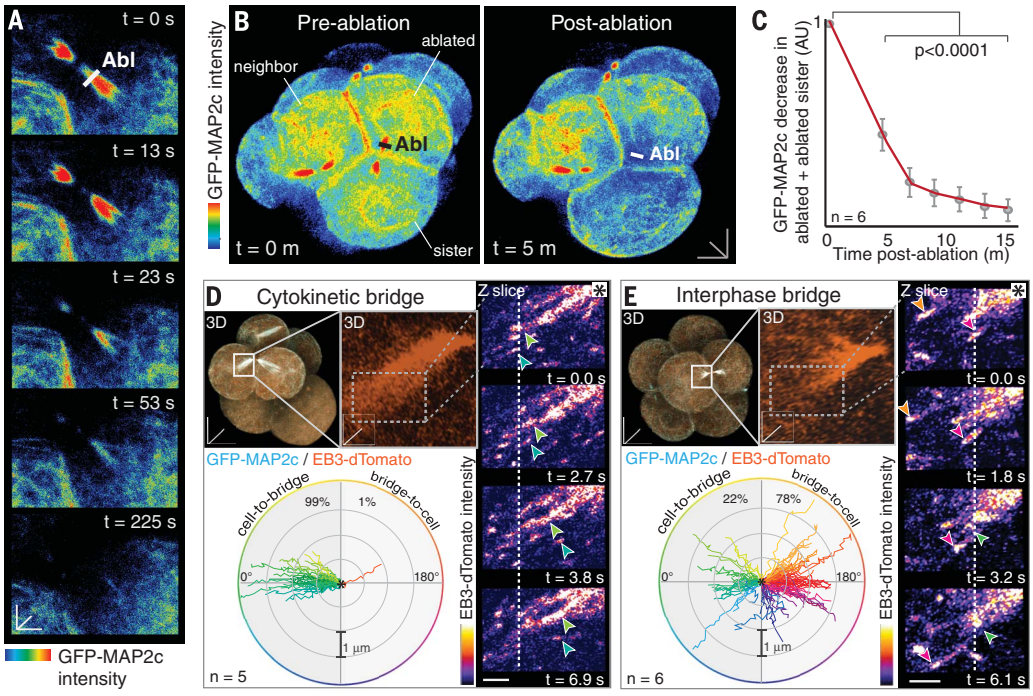

Fig. 2. The interphase bridge is an MTOC. (**A**) Live imaging shows MT depolymerization along the interphase bridge after laser ablation (Abl). (**B**) Live embryo demonstrates overall MT loss within the ablated cell and its sister, but not in the neighbor cell, post-ablation. (**C**) Reduction in GFP-MAP2c intensity after ablation. n, number of embryos; AU, arbitrary units. Error bars represent SEM. (**D** and **E**) Tracking MT plus ends labeled by EB3-dTomato at cytokinetic and interphase bridges. Images show bridges where tracking was performed. Arrowheads show MT plus ends moving within the confocal plane. Graphs show all tracks colored according to their endpoint angle relative to the longitudinal bridge axis. Asterisks mark the middle of bridges. Vertical dashed lines provide landmarks for comparison. The interphase bridge shows more MT plus ends projecting in a bridge-to-cell direction. Scale bars, 10 µm in images of entire embryos; 2 µm in all other images.

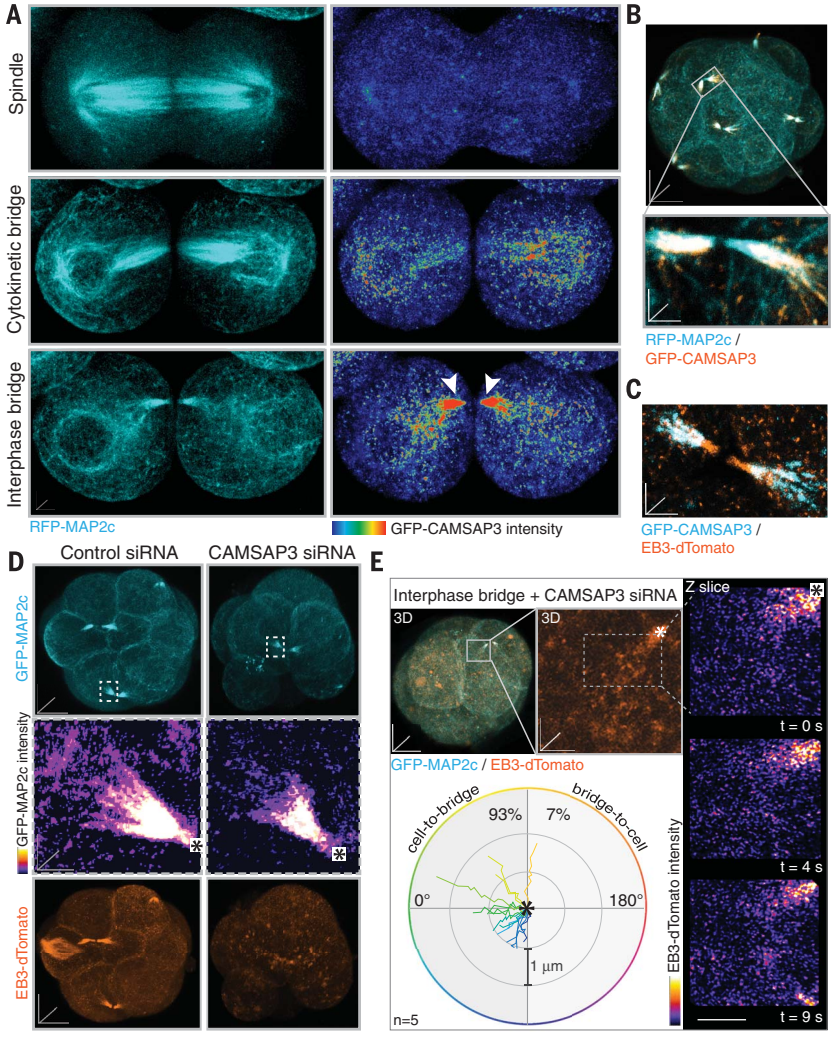

Fig. 3. CAMSAP3 enables the interphase bridge to function as a noncentrosomal MTOC. (**A**) Live imaging demonstrates GFP-CAMSAP3 accumulation at the interphase bridge (arrowheads), but not at the cytokinetic bridge. (**B**) Live embryo and zoomed-in view of GFP-CAMSAP3 accumulation at the interphase bridge. (**C**) GFP-CAMSAP3 overlaps with EB3-dTomato. (**D**) CAMSAP3 knockdown embryos form smaller interphase bridges and display reduced GFP-MAP2c and EB3-dTomato intensity. Asterisks indicate the middle of the bridges. siRNA, small interfering RNA. (**E**) CAMSAP3 down-regulation reduces EB3-dTomato–labeled MT plus ends tracking toward the cell. Images show interphase bridges where tracking was performed. Right panels reveal a lack of MT plus ends tracking toward the bridge. Asterisks indicate the middle of the bridge. Scale bars, 10 µm in images of entire embryos; 2 µm in all other images.

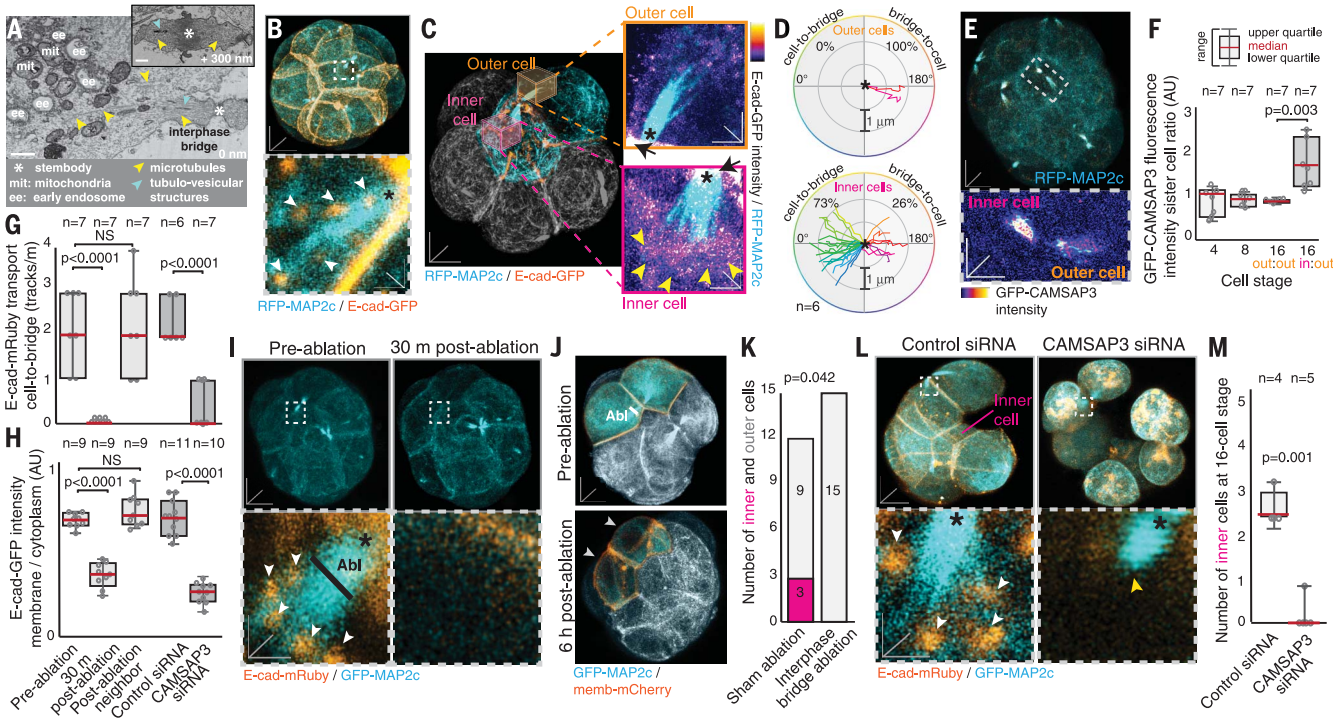

Fig. 4. The interphase bridge directs intracellular transport of E-cadherin. (**A**) Three-dimensional serial blockface scanning electron microscopy (3D-SEM) sections reveal vesicular structures near the interphase bridge. (**B**) Live embryo shows E-cad–GFP–labeled puncta (arrowheads) along the MTs of the interphase bridge. (**C**) E-cad–GFP is enriched at the interphase bridge of inner cells (arrowheads), compared with outer cells. Arrows show E-cad–GFP–labeled cell membranes. (**D**) Graphs show E-cad–GFP transport in inner and outer cells. Asterisks indicate the middle of the bridges. (**E** and **F**) GFP-CAMSAP3 is enriched in inner cells relative to outer cells. (**G** and **H**) Manipulation of the interphase bridge affects E-cad transport and localization. NS, not significant. (**I**) Laser ablation (Abl) of an interphase bridge eliminates transport of E-cad–mRuby puncta (arrowheads). (**J**) A cell with an ablated interphase bridge and its sister fail to undergo internalization (arrowheads). (**K**) Interphase bridge ablation disrupts inner-cell numbers. (**L**) CAMSAP3 down-regulation in half of the cells of the embryo disrupts E-cad–mRuby transport (white arrowheads) at the interphase bridge and inner-cell number. Knockdown embryos have smaller bridges (yellow arrowhead). (**M**) CAMSAP3 knockdown embryos have reduced inner-cell numbers. Asterisks indicate the middle of the bridge in (B), (C), (I), and (L). Scale bars, 1 μm for 3D-SEM; 10 μm in images of entire embryos; 2 μm in all other images.

photostatins (or photoswitchable inhibitors of MT polymerization, hereafter referred to as PSTs) (*19*). Moreover, MT outgrowth is rescued by PST deactivation with the use of 514-nm light (fig. S5, D to F, and movie S7). Together, these experiments show that the interphase bridge functions as an active MTOC.

We next determined how the interphase bridge stabilizes MT minus ends to enable MT outgrowth. The centrosomal markers ninein, γ-tubulin, and PCM1 (*20*) do not localize to the interphase bridge (fig. S6A). Furthermore, EB3-dTomato tracks project randomly near green fluorescent protein (GFP)–γ-tubulin foci, and γ-tubulin down-regulation does not affect MT outgrowth from the bridge or the overall MT network within the cell (fig. S6, B to F). However, live imaging reveals a marked accumulation of the noncentrosomal protein CAMSAP3 at the interphase bridge (Fig. 3, A and B; fig. S7, A to C; and movie S8). GFP-CAMSAP3 localization overlaps with EB3-dTomato (Fig. 3C), revealing that the interphase bridge contains MT plus and minus ends, like centrosomes in other cell types (*21*). Moreover, GFP-CAMSAP3 is undetectable at the cytokinetic bridge (Fig. 3A), consistent with its lack of MT outgrowth (Fig. 2D and movie S5).

We do not exclude that CAMSAP3 might stabilize MTs in other parts of the cell. However, the interphase bridges of CAMSAP3 knockdown embryos are smaller and display reduced GFP-MAP2c and EB3-dTomato labeling (Fig. 3D and fig. S7, D to G, K, and L) and minimal MT outgrowth (6.7 ± 3.3% of EB3 trajectories project in a bridge-to-cell direction) (Fig. 3E, fig. S7J, and movie S9). Furthermore, CAMSAP3 knockdown cells show reduced overall MT density and polymerization (fig. S7, H and I). Therefore, the interphase bridge is a noncentrosomal CAMSAP3-dependent site of MT stabilization and growth.

We next used three-dimensional serial blockface scanning electron microscopy (3D-SEM) to address how the organization of MTs by the interphase bridge contributes to mammalian development. 3D-SEM reveals endosomes near MTs emanating from the interphase bridge (Fig. 4A and fig. S8). Furthermore, live imaging of a general membrane marker (memb-mCherry) demonstrates membranous structures tracking bidirectionally along the bridge (fig. S9A and movie S10), suggesting a transport function.

In nonmammalian systems, the cell adhesion molecule cadherin is transported in a dynein-dependent manner by Rab11 endosomes, toward sites of CAMSAP3/patronin (*22*–*24*). Whereas E-cadherin (E-cad) membrane localization in the mouse embryo is essential for cell adhesion and the allocation of cells to the pluripotent inner mass (*25*, *26*), its transport mechanisms remain unknown. Live imaging confirms colocalization of GFP-Rab11a–labeled puncta with E-cad–mRuby (fig. S9B). Moreover, these proteins are transported along MTs of the interphase bridge (Fig. 4B; fig. S9, C to E; and movie S10). GFP-tagged dynamitin, which is part of the dynactin-dynein MT minus-end–directed motor complex (*27*), is enriched at the interphase bridge but not at the cytokinetic bridge (fig. S9F). These results are consistent with MT minus-end–directed transport of Rab11a and E-cad toward a CAMSAP3-dependent MTOC.

Nocodazole treatment or dynein inhibition with ciliobrevin D (*28*) reduces E-cad–GFP transport and membrane localization (fig. S9, G, H, K, and L). Furthermore, a dominant-negative form of Rab11a (GFP-Rab11aDN) (*29*) reduces Rab11a transport (fig. S9I) and disrupts E-cad–mRuby membrane localization (fig. S9, J and L). Additionally, acute ectopic bridge abscission during interphase using the aurora B inhibitor Hesperadin (*30*) causes loss of all interphase bridges, followed by reduced

E-cad–mRuby transport and membrane localization (fig. S9, M to P). Therefore, E-cad is transported in a MT minus-end–directed and Rab11a-dependent manner, along the MTs of the interphase bridge.

As E-cad is essential for inner-cell allocation (*25*, *26*), we investigated differences in transport by the interphase bridge of inner and outer cells. Both E-cad and Rab11a are enriched at the interphase bridge of inner cells and display increased cell-to-bridge transport, relative to outer cells (Fig. 4, C and D, and fig. S10, A to D). These asymmetries in transport coincide with asymmetries in GFP-CAMSAP3 and RFP-MAP2c levels, and in bridge volume, between inner and outer cells (Fig. 4, E and F, and fig. S10, E and F). Furthermore, GFP-CAMSAP3 increase occurs concomitantly with the expansion of the basolateral surface area of internalizing cells (fig. S10, G to I).

Laser ablations targeting individual interphase bridges eliminate their transport of E-cad–mRuby and GFP-Rab11a puncta toward the cell membrane (Fig. 4, G and I, and fig. S11, A, E, and G). Furthermore, laser ablation reduces E-cad–mRuby intensity at basolateral membranes of the targeted cell, its sister, and the junctions shared with neighboring cells (Fig. 4H and fig. S11, B and C). Cell tracking shows that cells with ablated bridges fail to contribute to the inner mass (Fig. 4, J and K, and fig. S11D). In line with this, CAMSAP3 knockdown cells display reduced E-cad–mRuby and GFP-Rab11a transport at their interphase bridges and reduced E-cad–mRuby localization at the basolateral membrane (Fig. 4, G, H, and L, and fig. S11, F to H). Consistent with the loss of E-cad at the membrane (*25*, *26*), CAMSAP3 downregulation also causes defects in cell shape and inner-mass formation (Fig. 4, L and M, and fig. S11, I to L). Together, these results show that E-cad is transported to the basolateral membrane along MTs organized by the interphase MTOC, and this process is essential for early mammalian development (fig. S12).

In summary, we identify a noncentrosomal interphase MTOC directing E-cad transport in the early mouse embryo. Contrary to early views of spatially random MT organization (*5*, *6*), we reveal that the interphase bridge organizes nonmitotic MTs in the embryo (fig. S12). We propose that retention of the cytokinetic bridge after division provides a preexisting scaffold, enabling noncentrosomal MT stabilization and outgrowth. CAMSAP3 is not essential for the initial formation of the MT bridge, yet in its absence, this structure fails to convert into an MTOC, consistent with recent models of noncentrosomal MTOC assembly (*1*, *7*). The persistence of the interphase bridge throughout preimplantation development and its apparent presence in human embryos (*11*) suggest further functions. By connecting all sister cells, the bridge could provide mechanical coupling between cells and coordinate the spatiotemporal dynamics of cell division and polarization during early development.

REFERENCES AND NOTES

1. A. D. Sanchez, J. L. Feldman, *Curr. Opin. Cell Biol.* **44**, 93–101 (2017).
2. P. T. Conduit, A. Wainman, J. W. Raff, *Nat. Rev. Mol. Cell Biol.* **16**, 611–624 (2015).
3. D. Clift, M. Schuh, *Nat. Commun.* **6**, 7217 (2015).
4. C. Gueth-Hallonet *et al.*, *J. Cell Sci.* **105**, 157–166 (1993).
5. G. Schatten, C. Simerly, H. Schatten, *Proc. Natl. Acad. Sci. U.S.A.* **82**, 4152–4156 (1985).
6. K. Howe, G. FitzHarris, *Cell Cycle* **12**, 1616–1624 (2013).
7. A. Akhmanova, C. C. Hoogenraad, *Curr. Biol.* **25**, R162–R171 (2015).
8. W. Meng, Y. Mushika, T. Ichii, M. Takeichi, *Cell* **135**, 948–959 (2008).
9. M. H. Johnson, B. Maro, *J. Embryol. Exp. Morphol.* **90**, 311–334 (1985).
10. G. M. Kidder, D. J. Barron, J. B. Olmsted, *Rouxs Arch. Dev. Biol.* **197**, 110–114 (1988).
11. K. Chatzimeletiou, E. E. Morrison, N. Prapas, Y. Prapas, A. H. Handyside, *Hum. Reprod.* **20**, 672–682 (2005).
12. B. Mierzwa, D. W. Gerlich, *Dev. Cell* **31**, 525–538 (2014).
13. A. Efimov *et al.*, *Dev. Cell* **12**, 917–930 (2007).
14. J. L. Feldman, J. R. Priess, *Curr. Biol.* **22**, 575–582 (2012).
15. A. Khodjakov, R. W. Cole, B. R. Oakley, C. L. Rieder, *Curr. Biol.* **10**, 59–67 (2000).
16. N. M. Wakida, E. L. Botvinick, J. Lin, M. W. Berns, *PLOS ONE* **5**, e15462 (2010).
17. A. Akhmanova, M. O. Steinmetz, *Nat. Rev. Mol. Cell Biol.* **9**, 309–322 (2008).
18. M. Wieczorek, S. Bechstedt, S. Chaaban, G. J. Brouhard, *Nat. Cell Biol.* **17**, 907–916 (2015).
19. M. Borowiak *et al.*, *Cell* **162**, 403–411 (2015).
20. M. Bettencourt-Dias, D. M. Glover, *Nat. Rev. Mol. Cell Biol.* **8**, 451–463 (2007).
21. M. Piehl, U. S. Tulu, P. Wadsworth, L. Cassimeris, *Proc. Natl. Acad. Sci. U.S.A.* **101**, 1584–1588 (2004).
22. I. Khanal, A. Elbediwy, M. d. C. Diaz de la Loza, G. C. Fletcher, B. J. Thompson, *J. Cell Sci.* **129**, 2651–2659 (2016).
23. P. M. Le Droguen, S. Claret, A. Guichet, V. Brodu, *Development* **142**, 363–374 (2015).
24. J. G. Lock, J. L. Stow, *Mol. Biol. Cell* **16**, 1744–1755 (2005).
25. C. R. Samarage *et al.*, *Dev. Cell* **34**, 435–447 (2015).
26. R. O. Stephenson, Y. Yamanaka, J. Rossant, *Development* **137**, 3383–3391 (2010).
27. A. P. Carter, A. G. Diamant, L. Urnavicius, *Curr. Opin. Struct. Biol.* **37**, 62–70 (2016).
28. D. H. Roossien, K. E. Miller, G. Gallo, *Front. Cell. Neurosci.* **9**, 252 (2015).
29. M. Wilcke *et al.*, *J. Cell Biol.* **151**, 1207–1220 (2000).
30. P. Steigemann *et al.*, *Cell* **136**, 473–484 (2009).

ACKNOWLEDGMENTS

This work was supported by grants from the Deutsche Forschungsgemeinschaft (to J.Z. and O.T.-S.); the Swiss National Foundation and Human Frontier Science Program (to J.Z.); the National Health and Medical Research Council and Australian Research Council Centre of Excellence (to R.G.P.); the Centre for Nanoscience (to O.T.-S.); and A*STAR, the European Molecular Biology Organization, and Howard Hughes Medical Institute–Wellcome Trust (to N.P.). O.T.-S. is an inventor on patent application WO2015166295 submitted by Ludwig-Maximilians-University Munich that covers the structure of PST-1.

SUPPLEMENTARY MATERIALS

www.sciencemag.org/content/357/6354/925/suppl/DC1
Materials and Methods
Supplementary Text
Figs. S1 to S12
References (*31*–*33*)
Movies S1 to S10

7 February 2017; resubmitted 3 May 2017
Accepted 1 August 2017
10.1126/science.aam9335

Science

A microtubule-organizing center directing intracellular transport in the early mouse embryo

J. Zenker, M. D. White, R. M. Templin, R. G. Parton, O. Thorn-Seshold, S. Bissiere and N. Plachta

Science **357** (6354), 925-928.
DOI: 10.1126/science.aam9335

How microtubules organize in embryos

Cell functions ranging from cell division to morphogenesis rely on microtubules, with microtubule-organizing centers serving as anchoring sites for their outgrowth. Although the centrosome organizes the microtubule cytoskeleton in most animal cells, this organelle is absent in early development. Using live-cell imaging, Zenker *et al.* found that the cells of the early mouse embryo are connected by stable microtubule bridges to direct the growth of microtubules within them. Microtubules emanating from the bridges help to guide transport of key proteins, including E-cadherin, to the cell membrane to control cell polarization during early development.

Science, this issue p. 925